BEAM LOSS DUE TO FOIL SCATTERING IN THE SNS ACCUMULATOR RING*

J.A. Holmes and M.A. Plum, ORNL, Oak Ridge, TN, 37831, USA*

Abstract

In order to better understand the contribution of scattering from the primary stripper foil to losses in the SNS ring, we have carried out calculations using the ORBIT Code aimed at evaluating these losses. These calculations indicate that the probability of beam loss within one turn following a foil hit is $\sim 1.8\times10^{-8}\tau$, where τ is the foil thickness in $\mu g/cm^2$, assuming a carbon foil. Thus, for a typical SNS stripper foil of thickness $\tau = 390$ $\mu g/cm^2$, the probability of loss within one turn of a foil hit is $\sim 7.0\times10^{-6}$. This note describes the calculations used to arrive at this result, presents the distribution of these losses around the SNS ring, and compares the calculated results with observed ring losses for a well-tuned production beam.

INTRODUCTION

We present here the results of computational experiments aimed at evaluating prompt (within one turn) losses in the SNS ring due to scattering in the stripper foil, and we compare the calculated results with observed ring losses for a well-tuned production beam. We performed the calculations using the ORBIT Code [1]. The calculations consisted of injecting particles into the ring through the stripper foil, tracking them for a single turn, and then analyzing their fate. The injected distribution and location on the foil were taken to be those of the linac beam. Although the actual distribution of foil hits differs from this assumption, due to the circulating beam, the differences are at most a few millimeters or parts of a milliradian and are not considered here. We also made the foil artificially wide to ensure that no injected particles missed the foil. We employed the SNS ring lattice with production tunes $\nu_x = 6.23$ and $\nu_y = 6.20$. The beam energy was taken to be 925 MeV. In order to evaluate the losses, we included a complete set of limiting apertures around the ring. Because we are interested in losses due to foil scattering only, we performed single-particle tracking. Space charge and impedances were ignored. Two alternative settings of the ring injection kickers were used: 1) large kicks to give small betatron oscillations typical of the start of injection, and 2) small kicks to give large betatron oscillations typical of the end of injection.

The ORBIT Code contains four options for treating scattering from carbon stripper foils: 1) transparent foil (ignore scattering); 2) small angle Coulomb scattering only; 3) the full foil model with contributions from small angle Coulomb scattering, Rutherford scattering, nuclear elastic scattering, and nuclear inelastic scattering; or 4) the ORBIT collimation module with an appropriately thin carbon window. Options 3 and 4 contain the same physics [2] and differ only in method of access. Although the physics models in options 3 and 4 are identical, for historical reasons, the small angle Coulomb scattering contribution is formulated differently than in option 2. Option 2 was coded in ORBIT before the development of the collimator model, and it adopted the small angle Coulomb scattering model from the ACCSIM Code [3]. The collimator module uses the small angle and Rutherford scattering formulations presented in the textbook by Jackson [4]. The calculations presented here were carried out alternatively using each of these four methods. We applied both options 3 and 4, rather than simply option 3, as a consistency check and found the results to be in agreement. The assumed density of carbon in all these models is 2.265 g/cm^3, consistent with graphite, but because the results are presented for foil thicknesses in units of $\mu g/cm^2$, they are valid for diamond foils also.

Stripper foil model options 2-4 all involve Monte Carlo techniques and the use of random numbers. In its present implementation, we use the computer's clock time to seed the random number generator. Because of this the precise results vary from run to run, but by performing several "identical" calculations, the statistical accuracy of the results can be ascertained. We use 10^7 macroparticles in the calculations presented here, so that processes of 10^{-6} probability should occur ~10 times in our calculations.

RESULTS

The overall results of the calculations described in Section 1 are presented in Table 1. The first column describes the case. The first three cases assume a foil thickness of 390 $\mu g/cm^2$ and the last three cases assume an artificially high thickness of 18000 $\mu g/cm^2$. This seemingly arbitrary number is the thickness of the original SNS secondary stripper foil and, as such, it has been used in other studies. The 390 $\mu g/cm^2$ results were obtained by averaging over ten runs for each case. For each foil thickness, we present the results for 1) transparent foil (ignore scattering); 2) small angle Coulomb scattering only; and 3) the full foil model with contributions from small angle Coulomb scattering, Rutherford scattering, nuclear elastic scattering, and nuclear inelastic scattering. The performance of the calculations using the ORBIT collimation module, with an appropriately thin carbon window, essentially duplicated the full foil model results. The second and third columns show the number of macroparticles lost due to inelastic nuclear scattering and

* ORNL/SNS is managed by UT-Battelle, LLC, for the U.S. Department of Energy under contract DE-AC05-00OR22725.

ISBN 978-3-95450-118-2

due to total foil scattering, respectively, for a large injection bump similar to that at the beginning of injection. The fourth and fifth columns show these results for a smaller injection bump similar to that at the end of injection.

Table 1: Number of Macroparticles (of 10^7 Total) Lost in the First Turn Following Foil Scattering

Case	Initial Bump		Final Bump	
	Nuclear Inelastic	Total	Nuclear Inelastic	Total
390 μg/cm^2				
No scattering	0	0	0	0
Small angle Coulomb	0	36.6	0	33.9
Full scattering model	25.4	69.8	23.1	61.3
18000 μg/cm^2				
No scattering	0	0	0	0
Small angle Coulomb	0	1419	0	1342
Full scattering model	1173	3243	1089	3026

For both the 390 μg/cm^2 and 18000 μg/cm^2 cases, no particles are lost in the absence of foil scattering. For the case of small angle Coulomb scattering, no particles are lost due to nuclear inelastic scattering, but total losses of ~35 particles and ~1400 particles occur for the 390 μg/cm^2 and 18000 μg/cm^2 cases, respectively. We also see that slightly higher losses are registered with the initial bump than the final bump. This is counterintuitive because the final bump results in larger first turn betatron oscillations than does the initial bump (Fig. 1).

Putting all the information together, we can see that both for 390 μg/cm^2 or 18000 μg/cm^2, the following points can be made: 1) Because there are no losses when foil scattering is neglected, the observed losses here are caused by foil scattering; 2) Comparison of the small angle Coulomb scattering losses with the total losses indicates that small angle Coulomb scattering is responsible for roughly half of the total losses; 3) Comparison of the nuclear inelastic scattering losses with the total losses indicates that nuclear inelastic scattering is responsible for slightly more than one third of the total losses; 4) The remaining losses are presumably due to Rutherford scattering and nuclear elastic scattering; and 5) In all cases, losses are slightly higher with the initial bump than with the final bump. With respect to the second point, we must remember that the small angle Coulomb scattering model of option 2 is different from the model implemented in options 3 and 4.

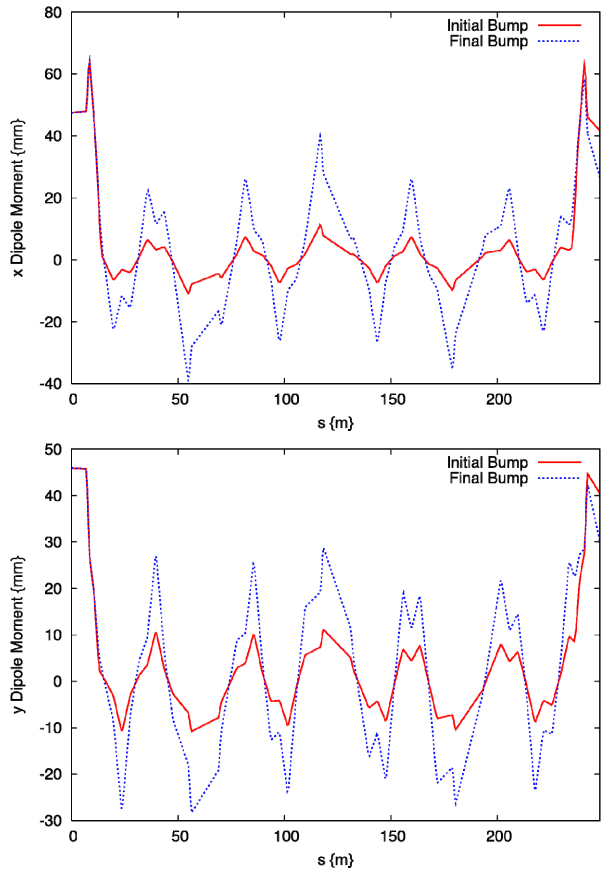

Figure 1: Horizontal (top) and vertical (bottom) beam orbits for first turn after foil hit with large (red, initial) and small (blue, final) closed orbit bumps. Note that these are first turn beam orbits, not the closed orbit.

Because all the loss mechanisms in Table 1 have very low probability, we expect the total losses to scale linearly with the foil thickness. To test this hypothesis, we divide the losses observed in Table 1 by the foil thickness used in their calculation, namely 390 for the 390 μg/cm^2 cases and by 18000 for the 18000 μg/cm^2 cases. We present these results in Table 2, in which we actually divide by 0.39 and by 18.0, respectively, thus normalizing the results to a foil thickness of 1000 μg/cm^2. Table 2 shows good agreement, within statistical error, between all the 390 μg/cm^2 cases and the 18000 μg/cm^2 cases, thus confirming the linear dependence of the losses on foil thickness. These results indicate that fractional losses are ~$1.8\times10^{-8}\tau$, where τ is the foil thickness in μg/cm^2, during the first turn following foil scattering. Of these, the losses due to small angle Coulomb scattering are ~$0.8\times10^{-8}\tau$ and ~$0.6\times10^{-8}\tau$ come from nuclear inelastic processes. We will now use the 18000 μg/cm^2 results with large (initial) bump size to describe the observed loss distributions.

ISBN 978-3-95450-118-2

Table 2: First Turn Foil Scattering Losses Normalized for Foil Thickness (to 1000 μg/cm2), Obtained by Dividing the 390 μg/cm2 Losses in Table 1 by 0.39 and the 18000 μg/cm2 Losses in Table 1 by 18.0.

Case	Initial Bump		Final Bump	
	Nuclear Inelastic	Total	Nuclear Inelastic	Total
390 μg/cm^2				
No scattering	0	0	0	0
Small angle Coulomb	0	93.8	0	86.9
Full scattering model	65.1	179.0	59.2	157.2
18000 μg/cm^2				
No scattering	0	0	0	0
Small angle Coulomb	0	78.8	0	74.6
Full scattering model	65.2	180.2	60.5	168.1

The loss distribution over the first turn following foil scattering is shown in Figure 2. The first plot was produced using the full foil scattering model (option 3), while the second plot was produced with the small angle Coulomb scattering model (option 2). The third plot shows experimental ring beam loss monitor (BLM) readings for a typical well-tuned production beam. With the full foil scattering model, most losses occur within the first 20 meters after the foil, but there are downstream losses, particularly in the collimation section (~50-60 m in the plot), in the extraction section (~130 m), and at the beginning of the injection chicane (~240 m). Although the plotted results are for the large injection bump, they are similar for both bump sizes. By comparing with the losses using the small angle Coulomb scattering model, we can infer that most of the downstream losses are due to small angle Coulomb scattering. Therefore, the Rutherford scattering and nuclear interaction losses occur mostly in the first 20 meters. Because the full foil scattering model in ORBIT removes beam particles immediately upon undergoing inelastic nuclear scattering, we identify these events with the first peak in the plots in Figure 2, which occurs precisely at the stripper foil. This peak does not exist when the small angle Coulomb scattering model is employed. The experimental BLM readings show a great deal of similarity to the loss results from the full foil scattering model. Although the losses are plotted versus BLM name in a bar graph, the initial peak occurs in the first 20 meters after the foil, the second area of activity is in the collimation region, there is a small reading directly following the extraction section, and the final activity occurs in the injection section upstream of the stripper foil. We now attempt a more quantitative analysis of these results.

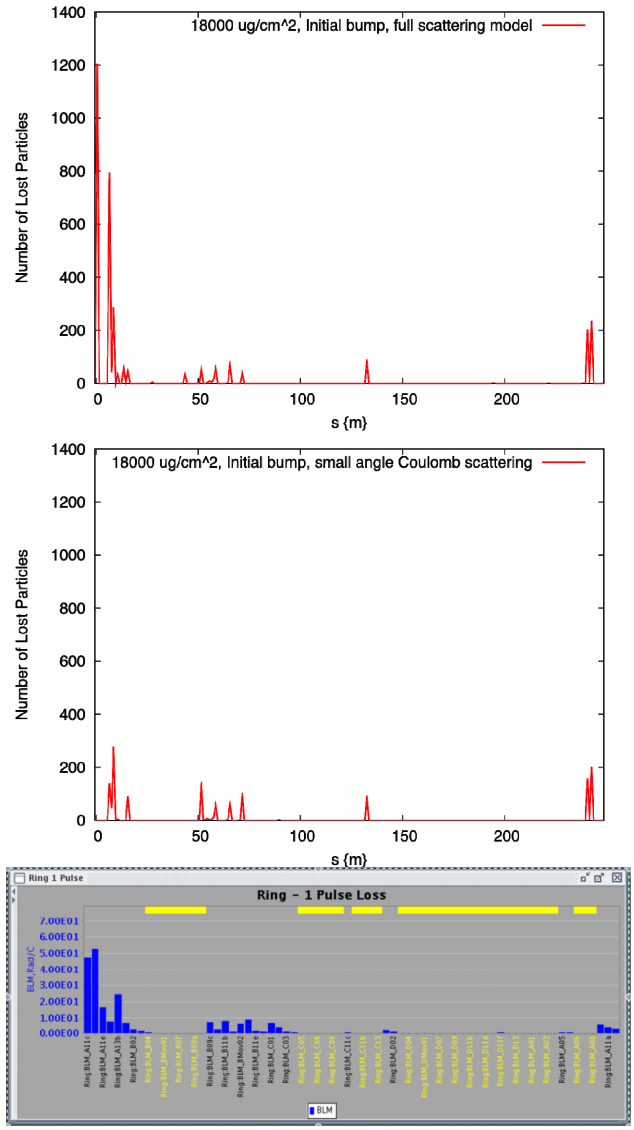

Figure 2: Loss distribution for first turn after foil scattering for full foil model (option 3, top) and for small angle Coulomb scattering (option 2, middle), together with experimental BLM readings for production tune (bottom).

ANALYSIS

In order to compare the calculated losses with the observed beam losses in the ring, it is necessary to convert them to the same units. Several years ago the ring BLMs were calibrated by spilling controlled amounts of beam at various locations around the ring and correlating the known beam losses with the BLM readings [5]. From this study, coefficients were derived to convert BLM readings into beam energy loss, which can in turn be converted to fractional beam loss. On the computational side, the results of Table 2 and Fig. 2 can be used to predict the

ISBN 978-3-95450-118-2

total beam loss and loss distribution due to foil scattering for any assumed number of foil hits per proton.

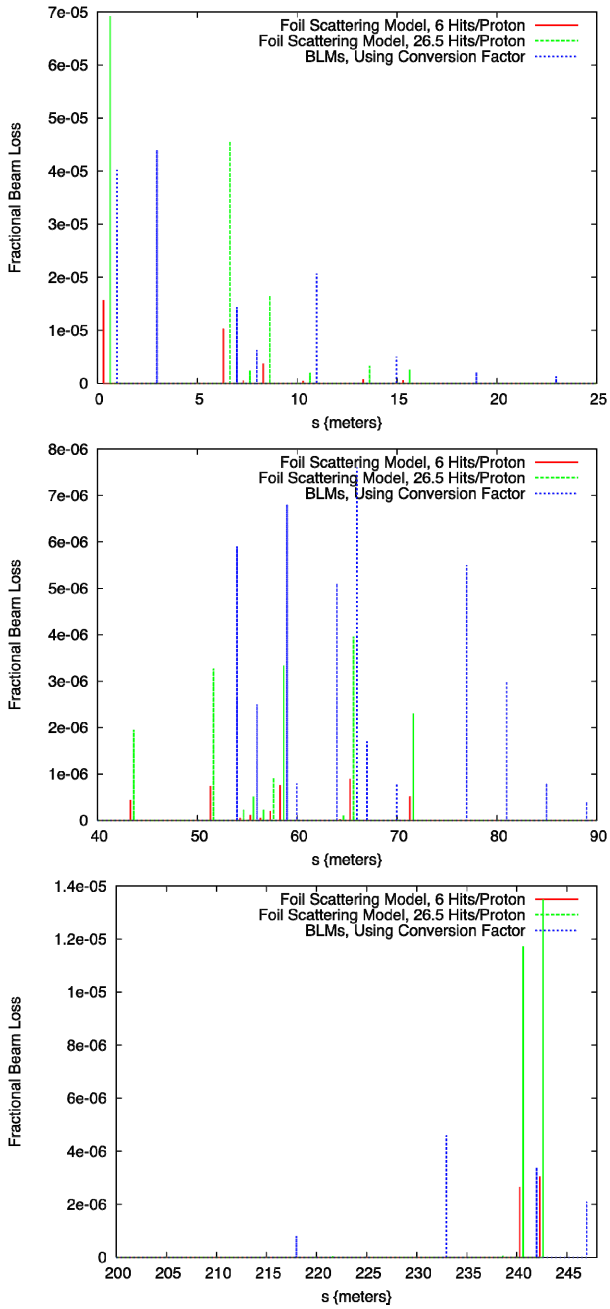

Figure 3: Fractional beam loss distributions comparing foil scattering model (red and green data) with observed BLM values (blue). Red lines were obtained assuming 6 foil hits per proton and green lines assume 26.5 foil hits per proton. The top plot is injection region downstream of foil, middle plot is collimation region, and bottom plot is upstream of foil.

Assuming a stripper foil of thickness 390 μg/cm^2, we converted the computed losses due to foil scattering to fractional beam losses, and using the experimentally derived BLM coefficients we converted the observed BLM signals to fractional beam loss. Figure 3 shows the resulting fractional beam loss distributions in various sections of the ring. The top plot shows the first 25 meters downstream of the stripper foil, which is the highest loss region in SNS. The center plot shows the region from 40 m to 90 m downstream of the stripper foil. It includes the collimation section, which is the second highest loss region in the ring. The bottom plot shows the region immediately upstream of the foil, which also has observable losses. In all three plots, the blue data denote the converted BLM readings shown in Fig. 2. According to the conversion factors and the known beam intensity of 18 μCoulombs and energy of 910 MeV, the total fractional beam loss is calculated to be 1.9×10^{-4}, with most occurring not far downstream of the foil. The red data were obtained from the calculations and an assumption of 6 foil hits per proton during accumulation. ORBIT simulations of SNS ring injection indicate that this is a likely number of foil hits. In this case, the fractional beam loss due to foil scattering is 4.3×10^{-5}, or about 23% of the experimental beam loss. The green data are the same as the red data, except that the values have been scaled to give the same fractional beam loss as the experiment, 1.9×10^{-4}. This would result from the foil scattering model with 26.5 foil hits per proton. This is almost certainly too many compared with the actual number, which is probably no higher than 10 foil hits per proton.

Let us compare the distributions of the model and experimental loss results. We focus on the green and blue data in Fig. 3, which are normalized to the same total loss. Most of the losses, both model and experimental, occur in the injection region, shown in the top plot. The dominant initial peak in the model losses comes entirely from nuclear inelastic scattering. Although ORBIT places all these losses at the location of the foil, in reality they are distributed over several meters downstream. Therefore, it is interesting that the sum of the first two experimental loss readings is comparable to the inelastic nuclear scattering peak in the model. Differences between the model losses and the observed losses occur between 6 m and 11 m downstream of the stripper foil. In the model, most of the losses in this region occur at the beginning of a quadrupole doublet about 7 meters downstream of the foil, while the experimental losses are divided between this location and a narrowing of the beam pipe about 11 m downstream. In spite of these detailed differences, both the model and the experimental results find that this is the highest loss region in the ring.

The middle plot in Fig. 3 shows the model and experimental losses in the collimation region, about one fourth of the way around the ring from the stripper foil. Although both the experiment and the model show this region to have the second highest losses in the ring, the BLM readings show higher losses than the does the foil model, even when 26.5 foil hits are assumed. This is perhaps not surprising because the experimental losses come from for the whole accumulating beam, and collective effects, magnet errors, and nonlinearities can contribute over many turns. Also, we expect losses due to

ISBN 978-3-95450-118-2

foil scattering to be most important in the injection region, not too far downstream of the foil.

Although not plotted in Fig. 3, both the foil model and the BLMs show some small loss in the extraction region about halfway around the ring from the injection foil. However, comparison of these values is not appropriate because the experimental losses are quite possibly due to beam in gap that is lost at extraction.

Finally, it is interesting and surprising that both experimental and model results show some beam loss upstream of the stripper foil, as shown in the bottom plot of Fig. 3.

SUMMARY AND DISCUSSION

We have carried out calculations using the ORBIT Code aimed at evaluating the contribution of foil scattering losses during the first turn following foil hits in the SNS accumulator ring. These calculations indicate that the probability of beam loss within one turn following a foil hit is $\sim 1.8\times10^{-8}\tau$ for carbon foils, where τ is the foil thickness in units of $\mu g/cm^2$. Thus, for a stripper foil of thickness $\tau = 390$ $\mu g/cm^2$, the probability of loss within one turn of a foil hit is $\sim 7.0\times10^{-6}$. According to the model, losses due to nuclear reactions and Rutherford scattering occur mostly in the first 20 meters following the foil, while losses due to small angle Coulomb scattering occur further downstream in the collimation and extraction sections.

We also compared the calculated losses from ORBIT's foil scattering model with experimentally measured losses from a well-tuned SNS beam. Using a likely estimate of an average of 6 foil hits per proton during accumulation, we estimated that foil scattering would account for about one fourth of the observed losses, a fractional rate of 4.3×10^{-5} compared to the experimental rate of 1.9×10^{-4}. An unlikely number of 26.5 foil hits per proton would be necessary to explain the total losses in terms of foil hits, if the foil scattering model and the BLM calibration coefficients are accurate.

However, there are a number of uncertainties present in this comparison. The BLM calibration coefficients obtained from experiment are not precisely known. It is difficult to control the exact locations for intentional beam spills, and variations in the actual and intended locations can affect the BLM readings, and consequently the calibration. Another uncertainty is the number of foil hits per proton. This number is sensitive to the actual injection painting and, although optimized ORBIT simulations usually predict about 6 foil hits/proton over the course of injection, the actual number could be higher. Finally, about 5% of the injected beam either misses the primary stripper foil or is incompletely stripped by it. A secondary stripper foil of thickness 1500-2000 $\mu g/cm^2$ subsequently strips these particles before they go to the injection dump. The associated losses can be estimated from the ORBIT model to be in the range $1.3\text{-}1.8\times10^{-6}$, a small contribution. Given the uncertainties discussed here, the level of agreement between the ORBIT calculations and the experimental measurement of the fraction and distribution of beam loss is reasonable. While further studies will be necessary to clarify the effect of the injection bump size, present results provide a useful estimate of the contribution of foil scattering to the observed losses in the SNS ring.

One future direction that we have begun to pursue is the estimation of the foil scattering losses in the injection region using the code G4beamline [6], which incorporates physics models from the Geant4 code together with accelerator beam line elements. With its sophisticated interaction models, G4beamline will provide further elucidation of the contribution of foil scattering to beam loss in the SNS ring.

REFERENCES

[1] J.A. Holmes, S. Cousineau, V.V. Danilov, S. Henderson, A. Shishlo, Y. Sato, W. Chou, L. Michelotti, and F. Ostiguy, "The ICFA Beam Dynamics Newsletter", Vol. 30, 2003.

[2] S. Cousineau, "Understanding Space Charge and Controlling Beam Loss in High Energy Synchrotrons", PhD Thesis, Indiana University (2003).

[3] F. Jones, "User's Guide to ACCSIM", TRIUMF Design Note TRI-DN-90-17, (1990).

[4] J.D. Jackson, "Classical Electrodynamics", Wiley and Sons, (New York, 1967).

[5] S. Cousineau, S. Assadi, J. Holmes, and M. A. Plum, "Proc. of the Particle Accelerator Conf. 2007 (PAC07)", (Albuquerque, NM, 2007), TUOBKI01, 703.

[6] T. Roberts, "G4beamline User's Guide", www.muonsinc.com/g4beamline/G4beamlineUsersGuide.pdf

ISBN 978-3-95450-118-2